

# Fermi LAT Measurements of the Gamma-Ray Emission from the Large Magellanic Cloud

Troy A. Porter\* and Jürgen Knödseder† for the *Fermi* LAT Collaboration

\*Santa Cruz Institute for Particle Physics, University of California, 1156 High Street, Santa Cruz 95064

†Centre d'Étude Spatiale des Rayonnements, CNRS/Université de Toulouse, PO Box 44346, 31028 Toulouse Cedex 4

**Abstract.** Apart from the Milky Way, the Large Magellanic Cloud (LMC) is the only other normal star-forming galaxy that was conclusively detected in high energy ( $> 100$  MeV)  $\gamma$ -rays by the Energetic Gamma Ray Telescope (EGRET) on the *Compton Gamma-Ray Observatory*. However, the sensitivity of EGRET was sufficient only to marginally resolve the LMC. We report on measurements of the  $\gamma$ -ray emission from the LMC by the Large Area Telescope (LAT) on the *Fermi* Gamma-ray Space Telescope. For the first time an externally viewed star-forming galaxy is well resolved in  $\gamma$ -rays. We discuss the distribution of the LMC diffuse emission as seen by the LAT and implications for cosmic-ray (CR) physics.

**Keywords:** gamma rays, cosmic rays, Fermi Gamma-Ray Space Telescope

## I. INTRODUCTION

The diffuse Galactic emission (DGE) is the dominant feature of the  $\gamma$ -ray sky. It is produced by interactions of CRs, mainly protons and electrons, with the interstellar gas (via  $\pi^0$ -production and Bremsstrahlung) and radiation field (via inverse Compton [IC] scattering). It is a direct probe of CR fluxes in distant locations, and may contain signatures of physics beyond the Standard Model, such as dark matter annihilation or decay. However, the interpretation of the DGE is complicated by the fact that a large number and variety of discrete sources of  $\gamma$ -rays can also contribute, thus blurring the distinction between individual CR acceleration sites and true diffuse emission processes.

Gamma rays from CR interactions with the interstellar medium are also expected from nearby galaxies, and indeed, the EGRET instrument on board the *Compton Gamma Ray Observatory* detected  $\gamma$ -ray emission from the LMC [1]. The LMC is an excellent target for studying the link between CR acceleration and propagation and diffuse  $\gamma$ -ray emission because of its proximity and its almost face-on orientation simplifies the interpretation of the diffuse emission versus the DGE. In addition, the LMC is host to many supernova remnants, bubbles and superbubbles, and massive star-forming regions that all are potential CR acceleration sites [2], [3], [4].

The LAT onboard the *Fermi* Gamma-ray Space Telescope provides significantly improved capabilities for in-

depth studies of the diffuse  $\gamma$ -ray emission from nearby galaxies, and of the LMC in particular [5], [6]. In this paper we report on the initial analysis of measurements of the diffuse  $\gamma$ -ray emission from the LMC taken in the course of the first year's all-sky survey by the LAT.

## II. DATA SELECTION AND ANALYSIS

The LAT is the primary instrument on *Fermi* which was launched from Cape Canaveral on June 11, 2008. The LAT is an imaging, wide field-of-view, high-energy  $\gamma$ -ray telescope, covering the energy range  $\sim 20$  MeV to  $> 300$  GeV, that operates according to the pair-conversion principle and is instrumented with a precision tracker and calorimeter, each consisting of a  $4 \times 4$  array of 16 modules, a segmented anti-coincidence detector (ACD) that covers the tracker array, and a programmable trigger and data acquisition system. The LAT has a large  $\sim 2.4$  sr field of view, and compared to earlier  $\gamma$ -ray missions, has a large effective area ( $> 7000$  cm<sup>2</sup> on axis at  $\sim 1$  GeV for the event selection used in this paper), improved angular resolution ( $\sim 0.5^\circ$  68% containment radius at 1 GeV for  $\gamma$ -ray conversions in the thin-radiator section of the LAT) and low dead time ( $\sim 25$   $\mu$ s per event). The  $1\sigma$  energy resolution in the 100 MeV – 10 GeV energy range is better than  $\sim 10\%$ . Full details of the instrument, onboard and ground data processing are given in [7].

The data used in this work cover the period August 8th 2008 - April 24th 2009 and amounts to 211.7 days of continuous sky survey data taking. During this period a total exposure of  $\sim 2.3 \times 10^{10}$  cm<sup>2</sup> s (at 1 GeV) was accumulated for the LMC region.

### A. Data Preparation

The analysis presented in this paper was performed using the LAT Science Tools package, that is available from the *Fermi* Science Support Centre, with post-launch instrument response functions (IRFs, designated P6V3). Events for the data taking period mentioned above satisfying the standard low-background event selection (“Diffuse” events [8], [9]) and coming from zenith angles  $< 105^\circ$  (to greatly reduce the contribution by Earth albedo  $\gamma$ -rays) were used. To further reduce the effect of Earth albedo backgrounds, the time intervals when the Earth was appreciably within the field of view (specifically, when the centre of the field of view was

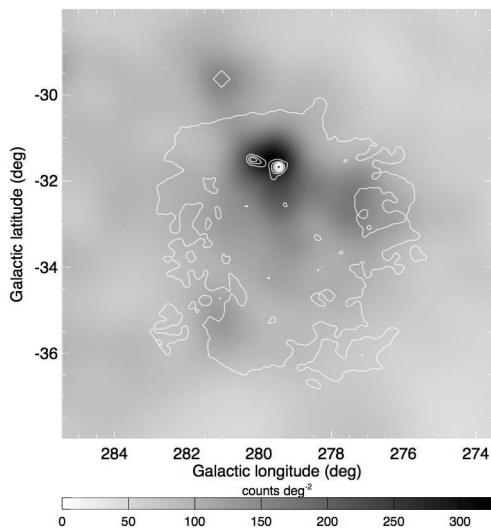


Fig. 1: Preliminary adaptively smoothed (s.n.r. = 10) LAT counts map of a  $10^\circ \times 10^\circ$  region centred on the LMC for the energy range 200 MeV – 100 GeV. Contours show the extinction map from [12] as an approximate tracer of the total gas column density in the LMC. Ten linearly spaced contour levels are plotted. The diamond in the north-east of the image designates the location of the blazar CRATES J060106-703606 [10] that contributes at a low level to the  $\gamma$ -ray emission in this area.

more than  $47^\circ$  from the zenith) were excluded from this analysis. We further restrict our analysis to photon energies  $> 200$  MeV where our current knowledge of the instrument response implies systematic uncertainties that are  $< 10\%$ .

### B. Morphology

Figure 1 shows a  $\gamma$ -ray counts map binned in  $3'$  pixels over a  $10^\circ \times 10^\circ$  area centred on the LMC. The exposure is very uniform across the region shown. The binned map has been smoothed using a two-dimensional adaptive Gaussian kernel technique [11] to reduce the effects of Poissonian noise. The signal-to-noise ratio (s.n.r.) has been set to 10 to reduce statistical noise variations below  $< 10\%$ . Also shown is an overlay of the extinction map taken from [12] (hereafter, SFD) which is a tracer of the total gas column density in the LMC. To first order, the extinction scales linearly with total gas column (note, the colour correction method used by [12] breaks down for the peak of the extinction map due to the massive HII region in the centre of 30 Doradus). A substantial fraction of the gas is in a small area to the north of the LMC at  $(l, b) \approx (279.5^\circ, -31.5^\circ)$  which coincides with the 30 Doradus star-forming region. The LAT-measured LMC  $\gamma$ -ray emission also peaks in this area. The  $\gamma$ -ray intensity in the 30 Doradus region exceeds  $\sim 300$  counts  $\text{deg}^{-2}$  while the intensity level in other regions of the LMC is  $\sim 120$  counts  $\text{deg}^{-2}$  (the

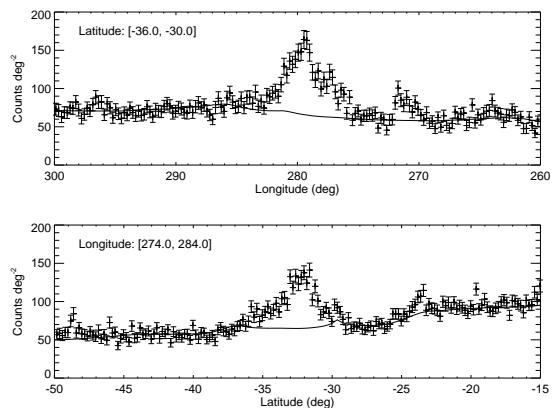


Fig. 2: Preliminary longitude (top) and latitude (bottom) photon intensity profiles of the LMC region for the energy range 200 MeV – 100 GeV. The solid line indicates the expected contributions from DGE, diffuse extragalactic emission, instrumental background and the blazar CRATES J060106-703606 at  $(l, b) = (281.04^\circ, 29.63^\circ)$  in this area of the sky.

background rate around the LMC is  $\sim 50 - 70$  counts  $\text{deg}^{-2}$ ).

The excess in the 30 Doradus region is also seen in the longitude and latitude profiles of the LAT-measured  $\gamma$ -ray intensity shown in Fig. 2. Within the rectangular region covering  $274^\circ \leq l \leq 284^\circ$  and  $-36^\circ \leq b \leq -30^\circ$  the net counts are  $\sim 1800$  in the energy range 200 MeV – 100 GeV above the expected contributions from DGE, extragalactic diffuse emission, residual charge-particle background, and the blazar CRATES J060106-703606 that was active for part of the data taking period. These background contributions have been estimated by fitting the data with spatial and spectral templates of the different components together with a spatial template for the LMC emission using a maximum likelihood method. The DGE has been modelled using the GALPROP code [14], [15] with a model corresponding to the GALDEF file 54\_59Xvarh7S<sup>1</sup>. For the combination of extragalactic diffuse emission and residual background we assumed an isotropic component with a power-law spectrum. CRATES J060106-703606 is modelled as a point source at  $(l, b) = (281.04^\circ, 29.63^\circ)$  with a power-law spectrum. For the LMC, we used the SFD extinction map as the spatial template. The average magnitude of the extinction map is obtained by averaging over all pixels outside a radius of  $4^\circ$  around  $(l, b) = (279.65^\circ, 33.34^\circ)$  within the rectangular region. For this figure, the pedestal value was subtracted from all pixels in the map. Then, all pixels outside of a radius of  $4^\circ$  centred on  $(l, b) = (279.65^\circ, 33.34^\circ)$  are set to zero in order to extract the LMC emission. For the LMC spectral model we assumed a power law.

To describe the morphology of the  $\gamma$ -ray emission

<sup>1</sup>Available from the website: <http://galprop.stanford.edu>

from the LMC we initially fit a point source with the position and flux free on top of the background model<sup>2</sup> to the data. This results in a best-fit point-source position  $(l, b) = (279.58^\circ, -31.72^\circ)$  with an error radius  $0.09^\circ$  95% confidence (statistical; the systematic position uncertainty is estimated to be  $< 0.02^\circ$ ). This position is close to the central star cluster of 30 Doradus, R136, located at  $(l, b) = (279.47^\circ, -31.67^\circ)$  which is  $\sim 0.11^\circ$  from our best-fit point-source location.

The detection significance of the LMC can be estimated using the so-called Test Statistic ( $TS$ ) which is defined as twice the difference between the log-likelihood,  $\mathcal{L}_1$ , that is obtained from fitting the LMC model on top of the background model to the data, and the log-likelihood,  $\mathcal{L}_0$  that is obtained by fitting the background model only,  $TS = 2(\mathcal{L}_1 - \mathcal{L}_0)$ . Under the hypothesis that our model satisfactorily explains the LAT data,  $TS$  follows a  $\chi_p^2$ -distribution with  $p$  degrees of freedom, where  $p$  is the number of free parameters in the LMC model [16]. For the case of a point source with position, flux, and spectral index free we obtain  $TS = 869.1$ .

We replaced the point source with an extended source model which was implemented as an axisymmetric two-dimensional Gaussian with variable angular size  $\theta$ . We redid the fit for position, flux, spectral index, and angular size and obtained a best-fitting source position  $(l, b) = (279.5^\circ, -32.3^\circ)$  (95% confidence radius  $0.1^\circ$ ) and source extent of  $\theta = 1.0^\circ \pm 0.1^\circ$ . The  $TS$  value is 1088.5 with a corresponding significance for source extension compared with the point source hypothesis of  $14.8\sigma$  ( $p = 5 - 4 = 1$ ).

TABLE I: Comparison of maximum likelihood model fitting results

LMC Model	$TS$	Number of Parameters
Point source	869.1	4
2D Gaussian source	1088.5	5
HI gas map	1173.4	2
CO gas map	932.2	2
HI + CO gas map	1176.1	4
SFD extinction map	1179.6	2
IRIS 100 $\mu\text{m}$ map	1179.1	2

In addition to the geometrical models we compared the LAT data to various spatial templates that trace the interstellar matter distribution in the LMC. For HI we use the aperture synthesis and multibeam data that [17] have combined from ATCA and Parkes observations. For  $\text{H}_2$  we use the CO observations of the LMC obtained with the NANTEN telescope [18]. We also used the SFD extinction map as tracer of the total gas column density and the 100  $\mu\text{m}$  IRIS map that has been obtained by reprocessing the IRAS survey data [19]. The results

<sup>2</sup>We call the combination of the GALPROP model, the isotropic model, and the CRATES J060106-703606 point source the “background model” for our analysis. The free parameters of this background model are the normalisation of the GALPROP model, the intensity and spectral slope of the isotropic component, and the flux and spectral slope of the CRATES J060106-703606 point source.

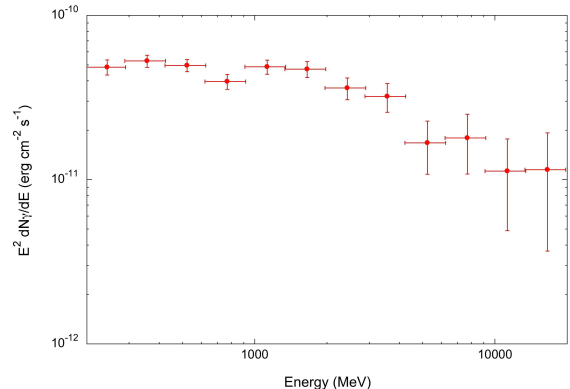


Fig. 3: Preliminary LMC spectrum obtained by fitting the extinction map from [12] in 12 logarithmically-spaced energy bins covering the energy range 200 MeV – 20 GeV to the LAT data. Note that errors are statistical only.

of this comparison are summarised together with that of the geometrical models in Table I. The best fits are obtained for the SFD extinction map and the IRIS 100  $\mu\text{m}$  map which give  $TS$  values of 1179.6 and 1179.1, respectively. For 2 free parameters (the total flux in the map and the spectral index) this corresponds to a detection significance of  $34.5\sigma$ . An almost equally good fit is obtained using the HI map. Fitting the CO map to the LAT data provides a poor fit, suggesting that the  $\gamma$ -ray morphology differs from that of molecular gas in the LMC. Fitting the HI and CO maps together confirms this result since  $\sim 97\%$  of the total flux is attributed to the HI component. The corresponding increase in  $TS$  with respect to simply fitting the HI map is negligible.

The HI/SFD/IRIS 100  $\mu\text{m}$  maps fit the data considerably better than a single point source, adding further evidence that the observed high-energy  $\gamma$ -ray emission is extended. Furthermore, the two-dimensional Gaussian source model is not as good as the tracer maps, suggesting that the emission morphology is more complex than a single Gaussian shape.

### C. Spectrum

Using the SFD extinction map (i.e., our best fitting spatial template of the high-energy emission) we extract a spectrum for the LMC by fitting the data in 12 logarithmically-spaced energy bins covering the energy range 200 MeV – 20 GeV. Above 20 GeV, photons from the LMC become too sparse in the data set used in this paper to allow for meaningful spectral points to be derived.

Figure 3 shows the LMC spectrum obtained by this method. Our analysis indicates a spectral steepening of the emission with increasing energy, suggesting a simple power law is an inadequate description of the data. We confirm this trend by fitting the data using a broken power law instead of a simple power law. This results in an improvement of the  $TS$  by 10.1

with respect to a simple power law, corresponding to a significance of  $2.7\sigma$  ( $p = 2$ ) for spectral steepening. Alternatively, fitting an exponentially cutoff power law improves the  $TS$  by 7.8 with respect to a simple power law, corresponding to a significance of  $2.8\sigma$  ( $p = 1$ ) for a spectral cutoff. Integrating either model over the energy range 100 MeV – 500 GeV gives identical photon fluxes of  $(3.1 \pm 0.2) \times 10^{-7}$  ph cm $^{-2}$  s $^{-1}$  and energy fluxes of  $(2.0 \pm 0.1) \times 10^{-10}$  erg cm $^{-2}$  s $^{-1}$  for the LMC. The systematic uncertainty in these flux measurements is  $\sim 10\%$ .

### III. DISCUSSION

The EGRET team [1] reported the initial detection of the LMC in high-energy  $\gamma$ -rays based on 4 weeks of data. Due to the limited angular resolution and sensitivity, the emission detected from the LMC was weak and details of the spatial structure of the galaxy were not resolved. However, it was obvious from the EGRET data that the LMC was an extended  $\gamma$ -ray source.

The LAT now clearly resolves the  $\gamma$ -ray emission from the LMC. The maximum of the emission is attributable to the massive star-forming region 30 Doradus. While this coincidence could be taken as a hint for an enhanced CR density in 30 Doradus with respect to the rest of the LMC, we note that a substantial fraction of the interstellar gas of the LMC is also confined to the 30 Doradus area. Consequently, the target density for CR interactions is greatly enhanced in this region which implies a corresponding enhancement of the  $\gamma$ -ray luminosity. In addition, the radiation field in this region is more intense due to the presence of significant numbers of massive, young stars, and this could also result in enhanced IC emission. Whether the data also support an enhanced CR density in 30 Doradus with respect to the rest of the galaxy requires further analysis.

The poor fit of the CO map to the LAT data suggests that the overall distribution of  $\gamma$ -ray emission differs from that of the H $_2$  in the LMC. The distribution of HI fits the data considerably better and the combined fit of HI and CO maps indicates that any contribution to the  $\gamma$ -ray emission that is correlated to the molecular gas is at best marginal. This agrees well with expectations since the gas budget of the LMC is largely (90-95%) dominated by HI [13]. Consequently we are presently unable to determine the CO-to-H $_2$  conversion factor,  $X_{CO}$ , from our LMC data.

Based on the assumptions of dynamic balance and that the electron/proton ratio in the LMC is the same as in the Milky Way [20] predicted a  $\gamma$ -ray flux  $> 100$  MeV for the LMC galaxy of  $F_{LMC}(> 100 \text{ MeV}) = 2.3 \times 10^{-7}$  ph cm $^{-2}$  s $^{-1}$ . More recently, [21] predicted a  $\gamma$ -ray flux  $> 100$  MeV  $F_{LMC}(> 100 \text{ MeV}) = 1.1 \times 10^{-7}$  ph cm $^{-2}$  s $^{-1}$  based on estimates of the LMC supernova rate and total gas densities. The flux measured by the LAT of  $(3.1 \pm 0.2) \times 10^{-7}$  ph cm $^{-2}$  s $^{-1}$  is greater than these model estimates. However, given the uncertainties in the models the agreement is satisfactory.

Further studies of the LMC with the LAT will concentrate on the spectral analysis of the data, placing particular emphasis on variations of the spectrum throughout the LMC. Due to the excellent sensitivity and angular resolution of the LAT this is the first time that such studies are possible. In addition, other nearby galaxies await detection as  $\gamma$ -ray sources, such as the Small Magellanic Cloud and the Andromeda Galaxy (M31). Both should be detectable by the LAT and the comparative study of their diffuse  $\gamma$ -ray emission will further our knowledge of CR physics in nearby galactic environments and ultimately our own Galaxy.

*Acknowledgements:* The *Fermi* LAT Collaboration acknowledges support from a number of agencies and institutes for both development and the operation of the LAT as well as scientific data analysis. These include NASA and DOE in the United States, CEA/Irfu and IN2P3/CNRS in France, ASI and INFN in Italy, MEXT, KEK, and JAXA in Japan, and the K. A. Wallenberg Foundation, the Swedish Research Council and the National Space Board in Sweden. Additional support from INAF in Italy for science analysis during the operations phase is also gratefully acknowledged.

### REFERENCES

- [1] P. Sreekumar, et al., *Astrophys. J.* **400**, L67 (1992).
- [2] C. J. Cesarsky & T. Montemerle, *Sp. Sci. Rev.* **36**, 173 (1983).
- [3] P. L. Biermann, *New. Astro. Rev.* **48**, 41 (2004).
- [4] W. R. Binns, et al., *Sp. Sci. Rev.* **130**, 439 (2007).
- [5] S. W. Digel, et al., *AIP Conf. Proc.* **528**, 449 (2000).
- [6] G. Weidenspointner, et al., *AIP Conf. Proc.* **921**, 498 (2007).
- [7] W. B. Atwood, et al., *Astrophys. J. in press* (2009).
- [8] T. A. Porter, et al., *this conference*, (2009).
- [9] A. A. Abdo, et al., *Phys. Rev. Lett.* *submitted* (2009).
- [10] S. E. Healey, et al., *Astrophys. J. Supp.* **171**, 61 (2007).
- [11] H. Ebeling, et al., *MNRAS* **368**, 45 (2006).
- [12] D. J. Schlegel, et al., *Astrophys. J.* **500**, 525 (1998).
- [13] Y. Fukui, et al., *PASJ* **51**, 745 (1999).
- [14] A. W. Strong, et al., *Astrophys. J.* **613**, 962 (2004).
- [15] T. A. Porter, et al., *Astrophys. J.* **682**, 400 (2008).
- [16] W. Cash, *Astrophys. J.* **228**, 939 (1979).
- [17] S. Kim, et al., *Astrophys. J. Supp.* **143**, 487 (2005).
- [18] R. Yamaguchi, et al., *PASJ* **53**, 959 (2001).
- [19] M. -A. Miville-Deschênes & G. Lagache, *Astrophys. J. Supp.* **157**, 302 (2005).
- [20] C. E. Fichtel, et al., *Astrophys. J.* **374**, 134 (1991).
- [21] V. Pavlidou & B. D. Fields, *Astrophys. J.* **558**, 63 (2001).